Universität Hamburg
DER FORSCHUNG | DER LEHRE | DER BILDUNG

Bachelor's Thesis

Validation of a new scheme for the calculation of absorption by CFC gases

submitted by

Hanna Dunke

Matriculation Number: 6764790
Hanna.Dunke@studium.uni-hamburg.de

Primary Referee: Prof. Dr. Stefan Bühler
Secondary Referee: Dr. Manfred Brath

November 2018

Universität Hamburg
MIN-Fakultät, Fachbereich Geowissenschaften
Meteorologisches Institut

Title: Validation of a new ARTS module for the calculation of absorption by CFC gases

Abstract

A new scheme implemented into the ARTS radiative transfer model which now includes the absorption of radiation by halocarbons is validated and new radiative forcing estimates for each gas are derived. Validation is based on the comparison of the forcing values to values from literature, the RRTMG and the LBLRTM model. A variety of possible assumptions underlying the model's calculations can have significant influence on the resulting radiative forcing. The inclusion of clouds, for example, could reduce the forcing value by up to 40 % depending on the gas. Therefore, a clear documentation of the radiative forcing calculations and the assumptions made is also part of this thesis.

The results of the comparison showed, that the forcing values for the main chlorofluorocarbons CFC-11, CFC-12 and CFC-113 were in good agreement with the reference values but overall slightly higher. Larger differences between the models were found for CCl_4 and CF_4. LBLRTM allowed the most-detailed comparison because the model type and atmospheric input data was identical. When comparing ARTS to LBLRTM we found that high deviations for CF_4 and CCl_4 were connected to large differences in the shape and size of the spectra. We were further able to determine a bug in the line data used by LBLRTM which caused additional discrepancy between the forcing values.

In total, most of the radiative forcing values derived with the new scheme are reasonable and only few gases cause larger uncertainties. Furthermore, the new state-of-the-art radiative transfer calculations indicate that radiative forcing values for the main chlorofluorocarbons may currently be underestimated.

List of Figures

List of Tables

Contents

Chapter 1

Introduction

When passing through the earth's atmosphere, a pencil of radiation can be modified in several ways which results either in an increase or a decrease of radiation. Emission for example always results in an increase of radiation as the atmosphere emits radiation as a grey body depending on its temperature and emission characteristics. Absorption is the counterpart of emission. As radiation passes through the atmosphere, a fraction of it is absorbed and the radiation is therefore decreased. The amount of absorption and emission in the atmosphere depends on its composition of different atmospheric gases. They essentially control the earth's radiation balance which is commonly known as the greenhouse effect. Each atmospheric gas has its own impact due to its quantum mechanical and chemical characteristics and contributes its own share to the greenhouse effect. When speaking of the greenhouse effect it is important to distinguish between the natural greenhouse effect and the potential human impacts on it, also known as the anthropogenic greenhouse effect.

The focus of this thesis is on the contribution of so-called chlorofluorocarbons (CFCs) to the anthropogenic greenhouse effect. CFCs are man-made gases which had their origin in the 1920s when they were mainly used as refrigerants or chemical solvents. Their manufacture and use were banned by the Montreal Protocol in 1989 but due to their long lifetime they still play a vital role in the temperature balance of earth's climate. On the one hand they cause the depletion of ozone in the stratosphere through chemical reactions. On the other hand they absorb and emit radiation itself which can be expressed in terms of radiative forcing. Radiative forcing describes the capacity of a gas to affect the radiative energy balance of the earth's climate system. It is essential to estimate the magnitude of radiative forcing by CFCs and the strength of the climate system's response in order to improve the accuracy of future climate model projections and to be able to trace back how big the CFC's impact on climate change has already been until today.

A new scheme is implemented into the Atmospheric Radiative Transfer Simulator (ARTS) (Buehler et al., 2005; Eriksson et al., 2011) which includes the absorption by chlorofluorocarbons and other halocarbons based on the up-to-date high-resolution transmission (HITRAN) molecular absorption database and is now to be tested and validated. ARTS is a line-by-line radiation model (more details in Chapter 3) used to simulate radiative transfer through the atmosphere which includes scattering as well as absorption and emission by several atmospheric gases. In this study the instantaneous, clear-sky radiative forcing (RF) of 6 different gases for present-day conditions are calculated with a Global Annual Mean (GAM) atmosphere derived from the Radiative Forcing Model Intercomparison (RFMIP). The calculated radiative forcings are then put into context by comparing the results to literature values and values derived by 2 other radiative transfer models, the Rapid Radiative Transfer Model (RRTMG) and the Line-By-Line Radiative Transfer Model (LBLRTM), for the same conditions. The main goal of this thesis is to provide an analysis of the results calculated by the new ARTS absorption model and to verify their plausibility.

Chapter 2

Radiative impact of atmospheric gases

This chapter introduces the basics of the radiative energy balance in the atmosphere and briefly explains how halocarbons influence this balance. Furthermore the concept of radiative forcing as well as its variability and further specification is described.

2.1 Absorption by atmospheric gases

The earth's atmosphere is continuously preventing harmful electromagnetic radiation from reaching the earth's surface by scattering, reflecting and absorbing the main part of the radiation on its way through the atmosphere. About 69 % of the incoming energy from the sun is absorbed at the Earth's surface or by the atmosphere (National-Research-Council, 2005). The focus in this thesis lays on the absorption of radiation by atmospheric gases and the significant part of energy that is thereby locked. The absorption process takes place on a molecular level. According to quantum mechanics, atoms and molecules have internal energy states and can only change distinctly between them (Petty, 2006). Internal energy can increase and decrease in different ways. Throughout the spectral range of ARTS, molecules and atoms cause the appearance of spectral lines, the emission and absorption lines. Absorption lines occur when an atom or molecule absorbs a photon with the energy equal to the gap between the current energy state and the next higher energy state and therefore jumps into a higher internal energy level. For emission lines it works the opposite way. Whether a spectral line appears as emission or absorption line also depends on the translational kinetic energy of molecules (i.e. temperature) and the radiative background. Since the energy of photons depends on the wavelength, the absorption and emission by atoms and

molecules does equally (Petty, 2006). However, absorption does not only occur at the precise wavelengths determined by the permitted energy transitions but also at nearby wavelengths, an effect which is known as line broadening (Petty, 2006). Depending on which of the 3 main mechanisms causes the broadening the resulting line shapes differ. First, every spectral line has a natural width arising from the Heisenberg uncertainty principle, but this is almost always negligible in comparison to the other 2 broadening effects. Second, thermal motions give each molecule a random Doppler velocity which causes absorption to be blurred over some range of wavenumbers. Finally, random collisions can perturb the energy levels of the molecules and the resulting cumulative effect is known as pressure broadening. Information about every individual absorption line such as the line position, the line shape and the line strength are determined by the quantum properties of the molecule, as well as the pressure, temperature and concentration of the gas and are stored in so-called absorption cross-sections. The absorption cross-section thus provides us with a "spectral fingerprint" for every molecule or in our case for every atmospheric gas. Nevertheless, it is highly complex to predict at which wavelengths a gas is most likely to absorb or emit during a transition. It therefore entails one of the biggest uncertainties in radiative transfer calculations and often causes difficulties to compare results from different models. The HITRAN spectroscopic database is the most complete and widely used database in which spectroscopic parameters and absorption cross-sections are stored and constantly updated based on laboratory measurements (Petty, 2006). This database is used as source for the absorption cross-sections of the newly included atmospheric gases in the ARTS radiative transfer calculations.

The general absorption process by atmospheric gases is the foundation for the well-known greenhouse effect. Absorption cross-sections for most greenhouse gases show that they absorb mainly at infra-red wavelengths (1–20 μm) and therefore are good absorbers for the terrestrial longwave radiation (Pinnock et al., 1995). The part of the terrestrial radiation that is absorbed by greenhouse gases is then re-emitted isotropically and thus leads to an increase in atmosphere and surface temperature.

2.2 Halocarbons and their influence on the earth's climate

The best known greenhouse gas is carbon dioxide (CO_2), even though there are far more potent greenhouse gases in the atmosphere such as methane (CH_4), nitrous oxide (N_2O) and several chlorofluorocarbons (CFCs) which will be the focus of this

thesis. Chlorofluorocarbons along with hydrofluorocarbons (HFCs), chlorocarbons and fluorocarbons are classified as halocarbons, a class of compounds that contain carbon and at least one halogen. They were mainly used for industrial purposes before their production and use were banned by the Montreal Protocol on Substances that Deplete the Ozone Layer in 1989 along with other gases including bromocarbons and halons (IPCC, 2007). Before CFCs were banned their abundance increased drastically within a few decades, e.g. for CFC-11 from zero concentration during pre-industrial times (until 1940) to 0.268 ppb during the peak time in 1992. Since then their concentration constantly decreased to 0.228 ppb in 2018 for CFC-11 (see Figure 2.1). The yearly abundance for CFC-11 and CFC-12, the most potent of the CFCs, based on measurement data from the National Oceanic and Atmospheric Administration (NOAA) is shown in Figure 2.1. Even though halocarbons were mainly emitted in the Northern hemisphere they are evenly distributed over both hemispheres (Martinerie et al., 2009). Reason for that is their overall long lifetime which allows them to mix well throughout the troposphere. This is why they are often referred to as well-mixed greenhouse gases.

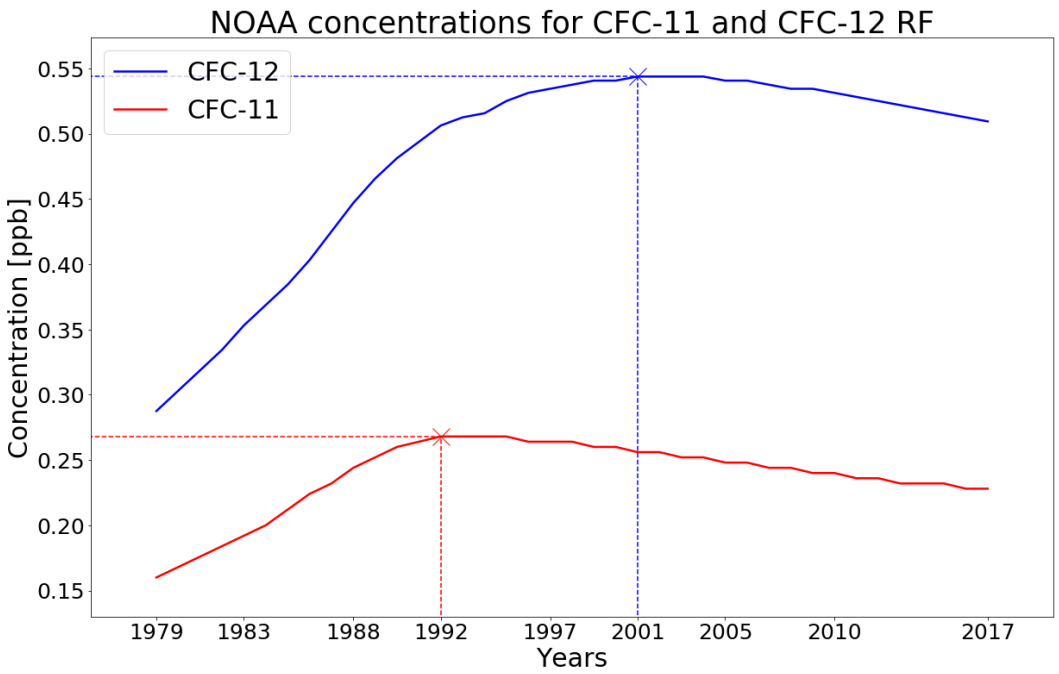

Figure 2.1: Global average CFC-11 and CFC-12 concentrations as yearly measured from the NOAA global air sampling network (Montzka and Butler, 2018). Abundances are plotted since the beginning of 1979 until today. The peak concentration values and the corresponding years are marked by the dotted lines.

Chlorofluorocarbons are synthetically produced and especially powerful greenhouse gases because they strongly absorb in the region of the electromagnetic spectrum where terrestrial infra-red (IR) radiation reaches its peak (Pinnock et al.,

1995). Bera et al. (2009) found that the IR absorption intensities within the IR atmospheric window (800–1400 cm^{-1}) are much larger than for example that of CO_2. The IR atmospheric window describes a region in the spectrum in which IR-radiation can pass directly to space without absorption and emission by natural greenhouse gases and therefore without heating the atmosphere. The fact that the CFC's absorption occurs mainly in this area boosted by their very long lifetime (up to 100 years for CFC-12 (see Table 2.1)) make them much more potent absorption agents compared to CO_2 on a per molecule basis (Bera et al., 2009).
Christidis et al. (1997) concludes that the actual contribution of a molecule to atmospheric absorbation depends on the amount emitted into the atmosphere, the molecule's atmospheric lifetime and its interaction with terrestrial infrared radiation which can be expressed in terms of the radiative forcing. Table 2.1 shows these characteristics for the radiatively active halocarbons which will be further investigated in this thesis based on the IPCC reports from 2001 and 2013. It is noticeably that HFC-134a is less stable than the CFCs and especially CF_4 which according to Singh et al. (2014) is due to reactions with the OH radical and other atmospheric agents in the troposphere. The lifetime of CFCs is comparably high because their only sink is the photolysis. During this chemical reaction photons with higher energy than the binding energy of a molecule cause a molecular vibration which eventually splits the molecule. Since the photolysis is only effective in the stratosphere and the CFCs are mostly chemically inert, they are extremely stable throughout the troposphere. Once they reach the stratosphere and photolysis is active they release halogen atoms which can then induce the breakdown of ozone (O_3) into oxygen (O_2).
In summary, CFCs unlike other halocarbons, affect the greenhouse effect in two different ways. On the one hand, they cause the depletion of ozone which affects the radiation balance in the stratosphere through indirect radiative forcing, and on the other hand they themselves absorb terrestrial infra-red radiation, thus also contributing to the direct radiative forcing. Due to their relatively small and constantly decreasing concentration they contribute relatively little to the total radiative forcing by greenhouse gases at present, but it is still important to accurately quantify the latter effect in order to analyse how past radiative forcing contributed to the observed historical global warming. It is therefore one main focus of this study to present updated state-of-the-art radiative forcing values for CFCs as well as the other halocarbons listed in Table 2.1.

Table 2.1: Radiative characteristics of several halocarbons as listed in IPCC (2013, 2001).

Gas	**Present day concentrations [ppt]**	**Atmospheric lifetime [years]**	**Radiative forcing [W/m^2]**
CFC-11	238±0.8	45	0.062
CFC-12	538±1	100	0.170
CFC-113	74.3±0.1	85	0.022
HFC-134a	62.7±0.3	13.6	0.010
CCl_4	85.8±0.8	35	0.015
CF_4	79.0±0.1	50000	0.004

2.3 Specification of radiative forcing definitions

A radiative forcing is according to IPCC (2013), "the net change in the energy balance of the Earth system due to some imposed perturbation". These perturbations can be caused by changes in concentrations of radiatively active gases such as CO_2 or the halocarbons listed in Table 2.1. Radiative forcings are usually defined as the top of the atmosphere (TOA) values expressed in watts per square meter and often present the value due to changes between two time periods (e.g. pre-industrial and present-day) (IPCC, 2013). The concept of radiative forcing provides a way to quantify and compare the contributions of different gases. At the same time they are straightforward to use in political and societal applications and thus provide a very useful metric for climate change research.
Over the past few years there has been a development of several definitions for radiative forcing. The assumptions underlying the calculations have a large impact on the final forcing value. It is therefore necessary that there is a scaling of literature values based on whether stratospheric adjustment is performed, whether clouds are included and which atmosphere data is used. Originally, radiative forcing values were defined as instantaneous forcings, representing the immediate change in the radiative energy balance at the TOA. The newer standard is the so-called adjusted forcing, which is the radiative forcing with consideration of stratospheric adjustment. Meaning, that the stratospheric temperature profile is allowed to adjust to the external perturbation and the stratosphere returns to a state of global mean radiative equilibrium. The stratosphere is a fast response system that reaches its equilibrium state on a much shorter time-scale than the surface-troposphere system and is largely decoupled from the surface. Halocarbons in the stratosphere for example absorb the upwelling radiation from

the troposphere and increase the heating rate of the stratosphere which causes the stratosphere to warm. The warming of the stratosphere causes an increase of the downward flux into the troposphere. Stratospheric adjustment therefore increases the radiative forcing values by up to 6 % compared to instantaneous forcing values (Jain et al., 2000). Hence it is more accurately for long-term forcings to be represented as adjusted forcings (Pinnock et al., 1995), focusing on the energy imbalance in the surface-troposphere system which is most relevant to surface temperature change.

Another important factor when assessing radiative fluxes is the influence of cloudiness. Clouds can scatter incoming shortwave radiation from the sun and therefore cause a global cooling. In addition, they increase the global reflection of shortwave radiation and cause an overall higher albedo. At the same time, however, they absorb and emit longwave radiation and can also have a warming effect. Consequently, cloud radiative forcing, the radiative impact of clouds, is negative for the shortwave component and positive for the longwave component (Calisto et al., 2014). In total, the energy loss through scattering and reflection mostly outweighs the gain leaving clouds with an overall cooling effect. The inclusion of clouds into the model therefore reduces the radiative forcing. According to the work of Pinnock et al. (1995), the impact can be as large as 35–40 %.

Table 2.2 based on Pinnock et al. (1995) and Jain et al. (2000) shows several radiative forcing values estimated with a narrowband model with a Global Annual Mean (GAM) atmosphere for a 0–1 ppbv increase in concentration. For the same gases, several of the above mentioned assumptions are made and the percentage deviations to the adjusted, cloudy-sky forcing values are presented. Table 2.2 emphasizes the need for a clear documentation of the assumptions made when radiative forcings are calculated. Furthermore it offers a possibility to compare values that are derived under different assumptions.

Table 2.2: Radiative forcings for a GAM atmosphere and a 0–1 ppbv concentration increase based on the work of Jain et al. (2000) and Pinnock et al. (1995). The percentage values can be interpreted as percentage offsets from the adjusted, cloudy-sky radiative forcing value.

Gas	**Adjusted/ Cloudy [W/m^2]**	**Adjusted/ Clear [%]**	**Instantaneous/ Cloudy [%]**	**Instantaneous/ Clear [%]**
CFC-11	0.269	+36.3	-6.4	+27.0
CFC-12	0.340	+33.5	-5.3	+28.2
CFC-113	0.319	+32.3	-3.6	+28.7
HFC-134a	0.181	+37.2	-7.2	+27.3
CCl_4	0.153	+28.2	-3.1	+25.1
CF_4	0.091	+26.6	-3.1	+23.5

Chapter 3

Calculation of radiative forcings for several halocarbons

This chapter briefly describes the radiative transfer calculations with ARTS. Additionally, all further steps towards the final radiative forcing values are documented and explained.

3.1 Radiative transfer calculations with ARTS

ARTS is an open-source line-by-line model used to perform simulations of atmospheric radiative transfer. Radiative transfer calculations are made using the general radiative transfer equation (Equation 3.1) which includes all processes (such as absorption, emission and scattering) that can decrease or increase radiation on its way through the atmosphere:

$$\frac{dI(\nu, r, n)}{ds} = -K(\nu, r, n) \cdot \mathbf{I}(\nu, r, n) + j_e(\nu, r, n) + j_s(\nu, r, n) \tag{3.1}$$

with

$$\mathbf{I} = \begin{bmatrix} I \\ Q \\ U \\ V \end{bmatrix} \tag{3.2}$$

The left part of Equation 3.1 can be interpreted as the change of the Stokes vector $\mathbf{I}$ along a distance s in the propagation direction n. On the right side, $\mathbf{K}$ represents the propagation or extinction matrix containing absorption and scatter-

ing effects, j_e is the thermal emission and j_s the scattering from other directions into the propagation direction. All 3 are functions of the frequency ν, the atmospheric position r and the propagation direction n (Buehler and Eriksson, 2017).
The Stokes vector **I** (Equation 3.2) consists of 4 different intensities, the full intensity of the radiation I, the difference between horizontal and vertical polarisation Q, the difference for $\pm 45°$ polarisation U and the difference for left and right circular polarisation V. With the aid of the Stokes vector the whole polarisation state of incoherent radiation or in other words the orientation of oscillations of electromagnetic waves (such as light) can be described (Buehler and Eriksson, 2017).
Radiative transfer calculations in ARTS can be made from any position along any direction through the model's atmosphere which can be either one- (1D), two- (2D) or three-dimensional (3D) (Eriksson et al., 2011). Radiative transfer is here performed for a set of monochromatic frequencies (depending on the input variable frequency grid) along pencil beam directions and the outcome of these calculations is the Stokes vector for each frequency whose dimension varies depending on the process considered. ARTS spectral range goes from the millimetre to the sub-millimetre range and thus covers mainly radiation from the microwave to the infra-red.

3.2 Flux calculations

Looking back at Table 2.2 from Section 2.3, we can see that it is very important to clearly state the assumptions made in the model before spectral fluxes and hence radiative forcings are derived. In the following section a step-by-step explanation is given of how the final radiative forcing values are calculated and which were the underlying assumptions.
The radiative transfer calculations are performed with ARTS (see Section 3.1) and all further calculations are made using the programming softwares Python and Typhon. One input-data required by ARTS is information about the atmospheric conditions. Atmosphere data from the Radiative Forcing Model Intercomparison Project (RFMIP) was used which contains temperature values and concentration data for atmospheric gases in 61 altitude levels. Since the focus is on present-day conditions only the first 100 atmosphere sets were extracted from the complete data, whereas "present-day" can be interpreted as the year 2014 (Pincus et al., 2016). Each atmosphere set has a profile weight w_i depending on its global position. In order to get a global and annual mean (GAM) atmosphere and forcing, which would be comparable to most literature values, the radiative forcings for the first 100 atmospheres were calculated and the weighted average was derived. The calculated radiative forcing as described in Section 2.3 is the change in net

irradiance flux. The direction for fluxes in ARTS is set positive for upwards fluxes and negative for downwards fluxes. In order to gain a better understanding of the following steps towards the final radiative forcing values a brief description of the radiative transfer calculation used for this set-up is necessary. A more detailed explanation of radiative transfer calculations by ARTS will not be a part of this thesis but can be found in Buehler et al. (2005) and the ARTS User guide (Buehler and Eriksson, 2017).

First of all, ARTS reads either the spectral line data or the absorption cross-sections from the HITRAN catalogue depending on the absorption species. One method to calculate absorption by atmospheric gases for example like water vapour and ozone is to use explicit line-by-line calculations. Another method which is used for the newly implemented halocarbons is to calculate their absorption by broadening of the cross section data from HITRAN and interpolating onto the current frequency grid. Using both methods ARTS generates a gas absorption lookup table. The idea of a lookup table is to pre-calculate absorption for a discrete number of combinations of variables (e.g. pressure, temperature, gas species concentration) and to adapt the table to the specific calculation by interpolation. A lookup table contains all information necessary to extract absorption data. The absorption data is then used for the radiative transfer calculations. In the calculation clear-sky conditions are assumed (particles are ignored) with no scattering. We can therefore simplify Equation 3.1 from Section 3.1. Without scattering the extinction matrix **K** contains only the extinction through absorption by species and the last scattering term in Equation 3.1 vanishes completely. Additionally, clouds and hence particles are not included in the calculation which leaves us with the following equation known as the Schwarzschild Equation:

$$\frac{\mathrm{dI}(\nu, \mathrm{r}, \mathrm{n})}{\mathrm{ds}} = -\mathbf{A}_{\mathrm{a}} \cdot \mathbf{I} + \mathrm{B} \cdot \mathrm{a}_{\mathrm{a}} \tag{3.3}$$

ν is the frequency, r the atmospheric position, n the propagation direction, s the distance along n, $\mathbf{A}_{\mathrm{a}}$ is the absorption vector for clear-sky calculations, **I** is the Stokes vector, B is the Planck function describing blackbody radiation (scalar value) and a_{a} is the first column of the absorption vector. There is no scattering and it is assumed that molecules don't have a preferred orientation which makes absorption unpolarised. Is that the case it is valid that only the first component of the Stokes vector (I=full intensity of the radiation) is considered and the dimension of the Stokes vector is set to 1. Equation 3.3 is solved numerically so that we get the one-dimensional Stokes vector per frequency or in our case the spectral radiance I [W/m^2·sr·Hz] which can be interpreted as intensity per solid angle and

frequency. Our spectral resolution is set to $0.1\,\mathrm{cm}^{-1}$ over a spectral range from $10\,\mathrm{cm}^{-1}$ to $3250\,\mathrm{cm}^{-1}$. This covers radiation from the thermal and mid-infrared to the far-infrared. The spectral radiances I are then integrated over the angle and frequency grid specified in ARTS in order to get the upwards and downwards irradiance flux L_{up} and L_{dn} [W/m^2] (see Equation 3.4). The net irradiance flux L_{net} [W/m^2] results from adding the upwards and downwards flux (see Equation 3.5) and is calculated for each of the following ARTS simulations:

- Full simulation including all CFC gases (baseline case)
- Simulation with CFC gas x concentration set to zero (experiment case)

The differences of the net fluxes for the full simulation and each simulation with one gas missing (see Equation 3.6) gives us the effect of each CFC gas. We are now left with net irradiance flux differences for each gas in 100 atmosphere profiles with each 61 vertical layers. From this the TOA values are extracted and the weighted mean as well as the weighted standard deviation are calculated using Equations 3.7 and 3.8. The result is the GAM instantaneous radiative forcing value for CFC gas x at the TOA.

$$L_{up/dn} = \int^{\nu} \int^{n} I \, dn d\nu \tag{3.4}$$

$$L_{net} = L_{dn} + L_{up} \tag{3.5}$$

$$RF_i = L_{net}(experiment) - L_{net}(baseline) \tag{3.6}$$

$$\overline{RF_x} = \sum_{i=1}^{100} w_i \cdot RF_i \tag{3.7}$$

$$\overline{std_x} = \sqrt{\sum_{i=1}^{100} w_i (RF_i - \overline{RF})^2} \tag{3.8}$$

Chapter 4

Results and discussion

The following chapter gives an overview of the results calculated by ARTS. In order to validate the new scheme implemented into ARTS, its reliability and applicability is checked by comparing the results to literature values and values derived by other radiative transfer models.

4.1 Results of radiative forcing calculations

Table 4.1 presents the radiative forcing values for several halocarbons calculated as described in Section 3.2. According to IPCC (1990) the form of the radiative forcing and concentration relationship depends primarily on the gas concentration. If you have low/moderate/high concentrations, the form can be approximated by a linear/square-root/logarithmic dependence of radiative forcing on concentration (IPCC, 2001). Since the concentration of halocarbons can be described as relatively low (see Chapter 2), a linear fit would be reasonable. The limit of this linear relationship is set to a concentration of 2 ppbv (IPCC, 1990). We can therefore assume that we have a linear relationship between radiative forcing and gas concentration for the CFCs calculated by ARTS. Consequently, we can linearly rescale the radiative forcing values in column 3 to reflect the impact for a 0–1 ppbv ($=$ 0–1$\cdot 10^{-9}$) increase in concentration. This is helpful when the results are compared to other studies because this is a common way of presenting radiative forcing values. The rescaled values can be found in column 4 of Table 4.1.

Before comparing the results from Table 4.1 we will have a look at the influence of temperature correction which is newly included into the scheme and considers the dependence of the absorption cross sections of gases on temperature and pressure. Christidis et al. (1997) announced the significance of including temperature dependent spectra to be very little with a percentage influence below 1 %.

Table 4.1: Table of radiative forcings for several atmospheric gases calculated with ARTS. The last column gives the linearly rescaled forcing values for a standard increase in concentration of 1 ppbv.

Gas	**Concentration [ppb]**	$\overline{\mathbf{RF}} \pm \overline{\mathbf{std}}$ **[W/m^2]**	$\overline{\mathbf{RF}} \pm \overline{\mathbf{std}}$ **[W/(m^2·ppbv)]**
CFC-11	0.2331	0.0941±0.0219	0.407±0.094
CFC-12	0.5206	0.2595±0.0653	0.498±0.125
CFC-113	0.0727	0.0347±0.0083	0.477±0.115
HFC-134a	0.0805	0.0212±0.0054	0.264±0.068
CCl_4	0.0831	0.0219±0.0045	0.264±0.054
CF_4	0.0811	0.0107±0.0027	0.133±0.034

The results of our own analysis can be found in Table 4.2. Column 4 in Table 4.2 shows the percentage deviation or percentage influence calculated with equation 4.2 from Section 4.2.2 for all included gases except CF_4. 4 of the 5 calculated deviations are below 1 %. Only for CFC-113 does the temperature correction seem to have a bigger influence. With this exception, our results agree well with the conclusion of Christidis et al. (1997) and we find the influence of the temperature correction to be negligible. We can therefore assume that the missing temperature correction for CF_4 won't have a significant effect on the resulting forcing value.

Table 4.2: Influence of the temperature correction (TC) in ARTS for 5 of the 6 included atmospheric gases.

Gas	**RF$_{\mathrm{ARTS}}$ with TC [W/m^2]**	**RF$_{\mathrm{ARTS}}$ without TC [W/m^2]**	**Deviation [%]**
CFC-11	0.0941±0.0219	0.0944±0.0220	0.32
CFC-12	0.2595±0.0653	0.2586±0.0651	-0.34
CFC113	0.0347±0.0083	0.0327±0.0080	-5.76
HFC134a	0.021227±0.005430	0.021223±0.005430	-0.02
CCl_4	0.0219±0.0045	0.0217±0.0044	-0.91

4.2 Comparison to literature

4.2.1 Comparison to the IPCC

There are basically two ways of calculating radiative forcing values. One is to run a radiative transfer model like ARTS but since the calculation of radiative forcings is rather computational expensive depending on the model type, it is very common to refer to empirical fits or "simplified expressions" as given by the Intergovernmental Panel on Climate Change in 1990 for several atmospheric gases (IPCC, 1990). These expressions for deriving adjusted radiative forcings were modified and presented again in 2001 with revised constants (see Table 4.3).

Table 4.3: Simplified expressions for the calculation of radiative forcing by CFC-11 and CFC-12. X is the concentration in ppb and X_0 unperturbed concentration in the year 1750, therefore X_0=0. The same expressions are used for all CFCs and CFC replacements, but with different values for α (see IPCC (2001)).

Gas	**Simplified expression: Radiative forcing ΔF [W/m^2]**	**Constants**
CFC-11	$\Delta F=\alpha(X\text{-}X_0)$	α=0.25
CFC-12	$\Delta F=\alpha(X\text{-}X_0)$	α=0.32

When comparing our values derived with ARTS (RF_{ARTS}) to the IPCC radiative forcing values (RF_{IPCC}) one has to keep in mind that the simplified expressions generate adjusted, cloudy-sky forcings as described in Section 2.3. According to Jain et al. (2000) and Pinnock et al. (1995) the IPCC values should be lower than the instantaneous, clear-sky forcings by about 27 % for CFC-11 and 28.2 % for CFC-12 (see Table 2.2). To compare the ARTS results to the IPCC values the instantaneous, clear-sky forcings from ARTS (RF_{ARTS}) for CFC-11 and CFC-12 are adjusted with percentage values from Table 2.2 using Equation 4.1. The results are shown in Table 4.4. One can see that the adjusted ARTS values ($RF_{adjusted}$) continue to be higher than the RF_{IPCC} but are well within the standard deviation. Even though this does not allow an extensive comparison one can get a first idea of how plausible the ARTS values are.

$$RF_{adjusted} = \frac{RF_{ARTS}}{1 + a} \tag{4.1}$$

4.2.2 Comparison to other studies

In addition to the previous comparison to IPCC values Table 4.5 shows a summary of radiative forcing values for several halocarbons derived in different studies.

Table 4.4: Adjustment of RF_{ARTS} values according to Pinnock et al. (1995) in order to compare them to RF_{IPCC} values from IPCC (2013). The adjustment percentage a can be understood as the percentage of the adjusted, cloudy-sky value.

Gas	**RF_{ARTS} [W/m²·ppbv]**	**Adjustment a [%]**	**$RF_{adjusted}$ (ARTS) [W/m²·ppbv]**	**RF_{IPCC} [W/(m²·ppbv)]**
CFC-11	0.407±0.094	27.0	0.320±0.074	0.261
CFC-12	0.498±0.125	28.2	0.381±0.098	0.322

During the 1990s there have been a lot of studies on the absorption and radiative forcing impacts by CFC gases and other halocarbons as possible replacements. However, only studies which calculated the radiative forcing under comparable assumptions were extracted, hence only for instantaneous and clear-sky conditions. This considerably limits the number of comparison values but at the same time increases the significance of the comparison. All comparison values were calculated using narrowband models (NBM) in contrast to ARTS which is a line-by-line model (LBLM). Due to high computational expenses it is common to use NBM rather than LBLM. Several studies also investigated the magnitude of difference in the radiative forcing values calculated by the two model types. Christidis et al. (1997), for example, found out that their narrowband model can indeed reproduce the line-by-line model quite well but differences of varying magnitude occur depending on the gases spectral features. We can therefore assume that the comparison of the ARTS values to NBM values is quite reasonable for the purpose of putting the newly derived radiative forcings into general context.
In order to gain a better idea of the significance of deviation between ARTS and the other values the percentage deviation using Equation 4.2 was calculated. RF_{study} is the forcing value from literature or later in Sections 4.3 and 4.4 the forcing value derived by each model. RF_{ARTS} refers to the radiative forcing values for each gas as listed in Table 4.1.

$$Deviation = \frac{RF_{study} - RF_{ARTS}}{RF_{ARTS}} \cdot 100 \tag{4.2}$$

The comparison of the radiative forcing values shows that the ARTS values tend to be slightly higher for the chlorofluorocarbons (CFC-11, CFC-12, CFC-113) but deviations stay below 20 %. The ARTS values for CFCs are in best agreement with the values from Jain et al. (2000) and Christidis et al. (1997) who both used a narrowband model with a spectral bandwidth of 10 cm^{-1}. The HFC-134a value is also in best agreement with Jain et al. (2000) whereas other comparisons show

discrepancies of up to 15.8 % for CF_4 and even up to 27.7 % for CCl_4. However, since the radiative forcing value from Jain et al. (2000) is the only available literature value for CCl_4 one can't draw any conclusions from this comparison. For all gases (except for CCl_4) the deviations of the ARTS value to the literature values lie well within the standard deviation of ARTS. The comparison therefore verifies the overall plausibility of the radiative forcing values derived by the new absorption scheme. However, one has to keep in mind that a certain magnitude of variations for all gases is bound to occur when one compares the results of different studies. The usage of different model types (e.g. broadband, narrowband or line-by-line models), as described above, as well as different spectroscopic and atmospheric data will naturally cause a certain discrepancy between the results. Furthermore, all of the studies are older than 12 years and the accuracy of spectroscopic data has widely improved since then. Nevertheless, the goal in this section was only to give the reader a general idea of the plausibility of the state-of-the-art ARTS values. A more precise comparison can be made in the following sections when the ARTS values are compared to the RRTMG and the LBLRTM model which are both run with the same atmospheric data.

4.3 Comparison to RRTMG

RRTMG is a narrowband radiative transfer model which calculates shortwave fluxes, longwave fluxes and cooling rates for application to general studies of atmospheric radiative transfer and for implementation into general circulation models. It is divided into sixteen contiguous bands in the longwave from $10\,cm^{-1}$ to $3250\,cm^{-1}$. The modeled molecular absorbers are water vapor, carbon dioxide, ozone, nitrous oxide, methane, oxygen, nitrogen and several halocarbons (CFC-11, CFC-12, CFC-22 and CCL_4). This allows the intercomparison of radiative forcing values for CFC-11, CFC-12 and CCL_4. Since the RRTMG values are calculated for instantaneous and clear-sky conditions using the same atmospheric data there is no need for scaling. Table 4.6 shows the values derived by ARTS in comparison to the radiative forcing values by RRTMG. The values for both chlorofluorocarbons are in good agreement, with a slightly higher deviation for CFC-11. While the ARTS values for the CFCs were constantly higher when compared to studies which used older spectroscopic data (see Section 4.2.2), they are now distinctly lower than the ones derived by RRTMG which, like ARTS, is based on newer spectroscopic data. It could therefore be a possibility that radiative forcing values for the 2 CFCs have been widely underestimated by radiative transfer models so far.
The deviation for CCL_4 in contrast is negative (meaning that the ARTS value is higher than the RRTMG value) and remarkably high. The forcing value by RRTMG

Table 4.5: Summary of radiative forcing values for several halocarbons from literature.

Gas	Study/ Reference	RF_{study} [W/(m^2·ppbv)]	Deviation [%]
CFC-11	**ARTS (2018)**	**0.407±0.094**	
	Pinnock et al. (1995)	0.342	-16.0
	Jain et al. (2000)	0.356	-12.5
	Christidis et al. (1997)	0.353±0.022	-13.3
	Sihra et al. (2001)	0.328	-19.4
CFC-12	**ARTS (2018)**	**0.498±0.125**	
	Jain et al. (2000)	0.436	-12.4
	Myhre et al. (2006)	0.400	-19.7
CFC-113	**ARTS (2018)**	**0.477±0.115**	
	Jain et al. (2000)	0.411	-13.8
HFC-134a	**ARTS (2018)**	**0.264±0.068**	
	Pinnock et al. (1995)	0.230	-12.9
	Jain et al. (2000)	0.278	+5.3
CCl_4	**ARTS (2018)**	**0.264±0.054**	
	Jain et al. (2000)	0.191	-27.7
CF_4	**ARTS (2018)**	**0.133±0.034**	
	Jain et al. (2000)	0.112	-15.8
	Sihra et al. (2001)	0.135	+1.5

is even lower than the one derived by Jain et al. (2000) from Table 4.5. Since the values of both models for the 2 CFCs were in quite good agreement this raises the question whether there might be a significant difference in the spectral data of CCl_4 that could be the reason for the big disagreement amongst the models. A question which could not be further investigated within the scope of this thesis.

Table 4.6: Radiative forcings for 3 atmospheric gases calculated with the RRTMG model (instantaneous, clear-sky).

Gas	**ARTS conc. [ppb]**	**RF_{ARTS} [W/m^2]**	**RF_{RRTMG} [W/m^2]**	**RF_{RRTMG} [W/(m^2·ppbv)]**	**Deviation [%]**
CFC-11	0.2331	0.0941±0.0219	0.1062±0.0300	0.4556±0.1286	12.9
CFC-12	0.5206	0.2595±0.0653	0.2823±0.0816	0.5422±0.1567	8.8
CCl_4	0.0831	0.0219±0.0045	0.0127±0.0034	0.1530±0.0412	-42.0

4.4 Comparison to LBLRTM

4.4.1 Results

LBLRTM is an often-used, efficient and flexible line-by-line radiative transfer model that includes all significant molecular absorbers. It uses spectral parameters based on HITRAN 2004 data. LBLRTM is a line-by-line model like ARTS which uses the same atmospheric data from RFMIP so that the radiative forcing values can be derived in the same way as the ARTS values (see Section 3.2) resulting in instantaneous, clear-sky GAM radiative forcings which offer the best possible comparison to the ARTS values.

The comparison of values in Table 4.7 shows that the radiative forcing values for the main CFCs, CFC-11, CFC-12, as well as for CFC-113 are in good agreement. The percentage error is below 10 % and all global mean values lie well within the standard deviation of each other. The results show further that even though the models use the same atmospheric input data and calculate fluxes over the same spectral range the forcing values differ by up to 32 % for the other halocarbons. Figure 4.1 shows the radiative forcing values calculated by both models for each gas and all 100 atmospheres in comparison. The overall good agreement for the CFC gases is identifiable. The forcing values for gases with higher deviations, hence CCl_4 and CF_4, spread more widely. In order to see the distribution of the atmospheres with the highest deviations between the two models their position is plotted on a world map, coloured differently depending on the magnitude and sign of the deviation (see Figures 4.2 to 4.5). Once again, when looking at the maps

for each gas, one can notice a similar pattern for CFC-11 and CFC-12 and more significant differences for the other halocarbons. The CFC-11 and CFC-12 forcing values derived by ARTS are overall slightly higher than the LBLRTM values whereas the deviations are lower in the equatorial zone and increase towards the mid-latitudes and poles. The magnitude of the deviations lies within 20-30 % of the ARTS forcing value for both gases (see Figures 4.2 and 4.3). Figure 4.4 for CCl_4 shows the same pattern of the smallest deviations near the equator and high deviations towards the poles but with a higher magnitude of maximum 54 % of the ARTS value. The gases CFC-113 and CF_4 show the opposite pattern. In almost all cases the sign of deviations for both gases is negative, which means that almost everywhere the LBLRTM forcing values are higher than the ARTS values. Furthermore, the highest magnitude of deviations occurs in the equatorial zone and the difference between the models decreases towards the poles. Even though they show the same pattern, the magnitude of deviation for CFC-113 is far lower (about 40 % at most) than the one for CF_4 which reaches deviations up to 81 % of the ARTS forcing value (see Figure 4.6 and Figure 4.5).

Table 4.7: Comparison of RFs calculated by ARTS and LBLRTM (instantaneous, clear-sky). The last column presents the percentage error between the 2 models for each gas.

Gas	$\mathbf{RF_{ARTS}}$ **[W/m^2]**	$\mathbf{RF_{ARTS}}$ **[W/(m^2·ppbv)]**	$\mathbf{RF_{LBLRTM}}$ **[W/m^2]**	$\mathbf{RF_{LBLRTM}}$ **[W/m^2·ppbv]**	**Deviation [%]**
CFC-11	0.0941±0.0219	0.407±0.094	0.0873±0.0238	0.374±0.102	-7.3
CFC-12	0.2595±0.0653	0.498±0.125	0.2389±0.0668	0.459±0.128	-7.9
CFC-113	0.0347±0.0083	0.477±0.115	0.0381±0.0117	0.524±0.161	9.8
CCl_4	0.0219±0.0045	0.2635±0.0539	0.016±0.005	0.194±0.060	-26.3
CF_4	0.0107±0.0027	0.1325±0.0337	0.014±0.005	0.175±0.062	32.1

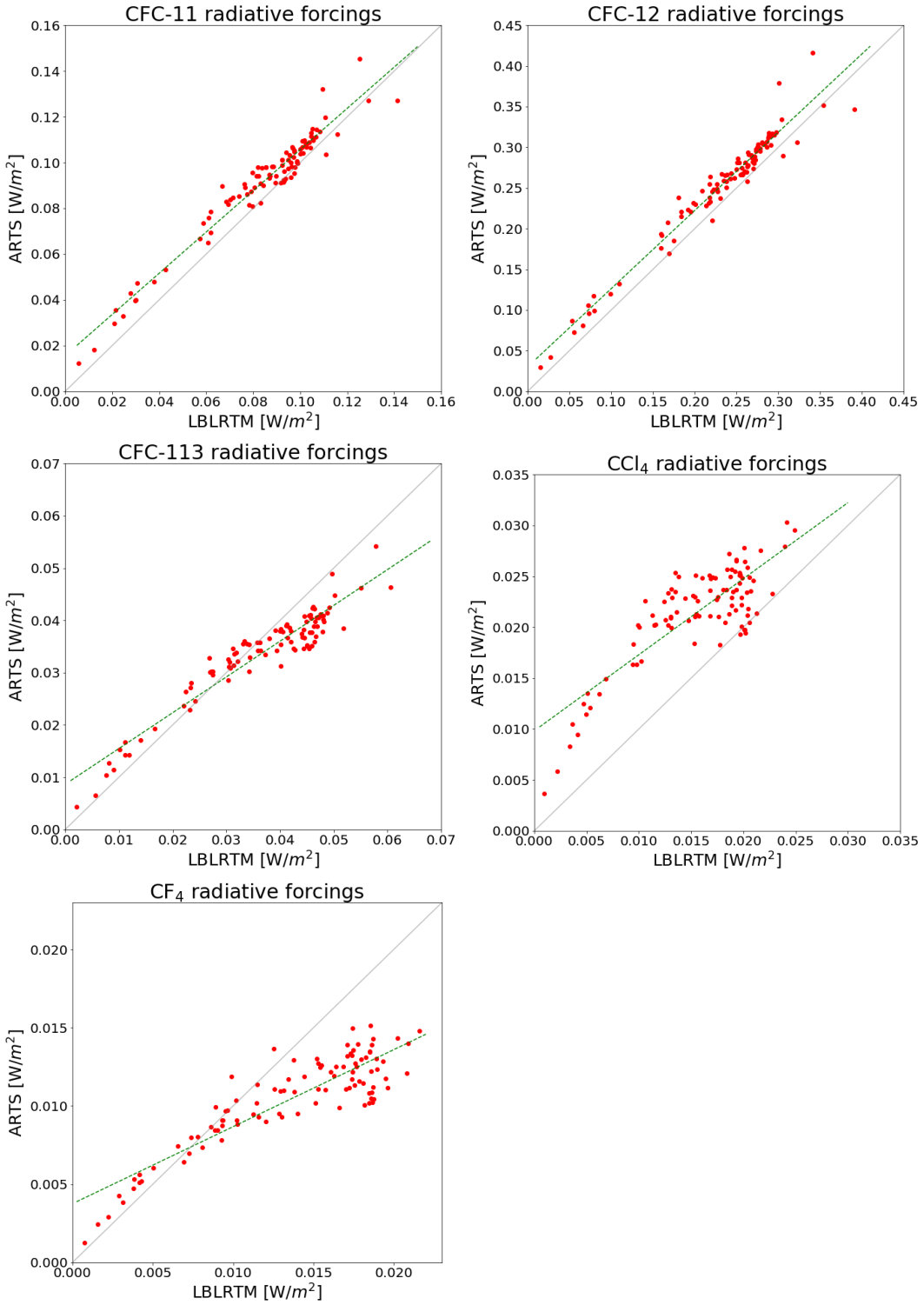

Figure 4.1: Comparison of radiative forcings for 5 atmospheric gases calculated with ARTS and LBLRTM. Each red dot represents the forcing values for one of the 100 atmospheres. The green dotted line is the linear regression of the values whereas the gray one is the 45 degree line.

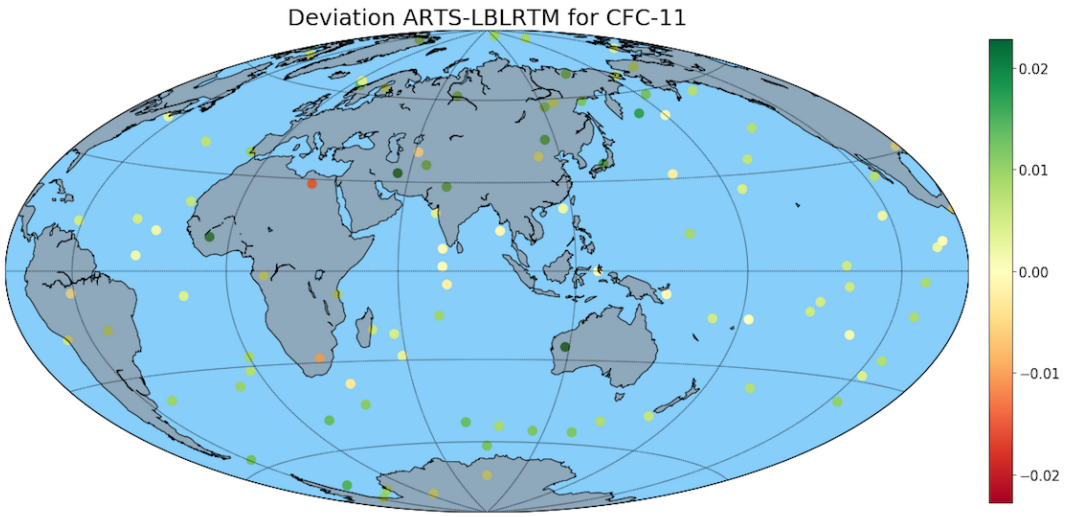

Figure 4.2: Worldmap showing the geographic position of the atmosphere data each colored differently depending on the magnitude of deviation between the ARTS and LBLRTM value for CFC-11.

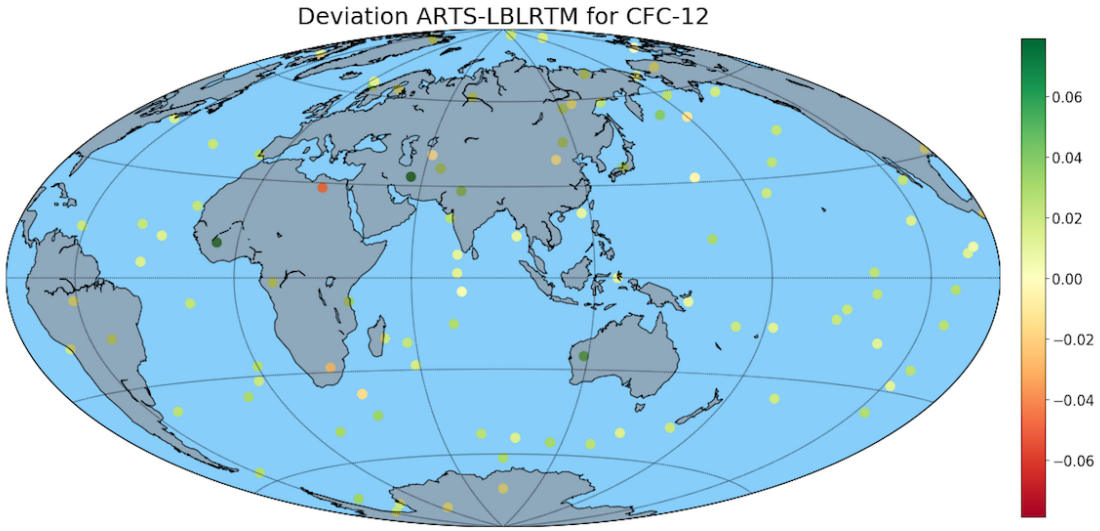

Figure 4.3: Worldmap for CFC-12.

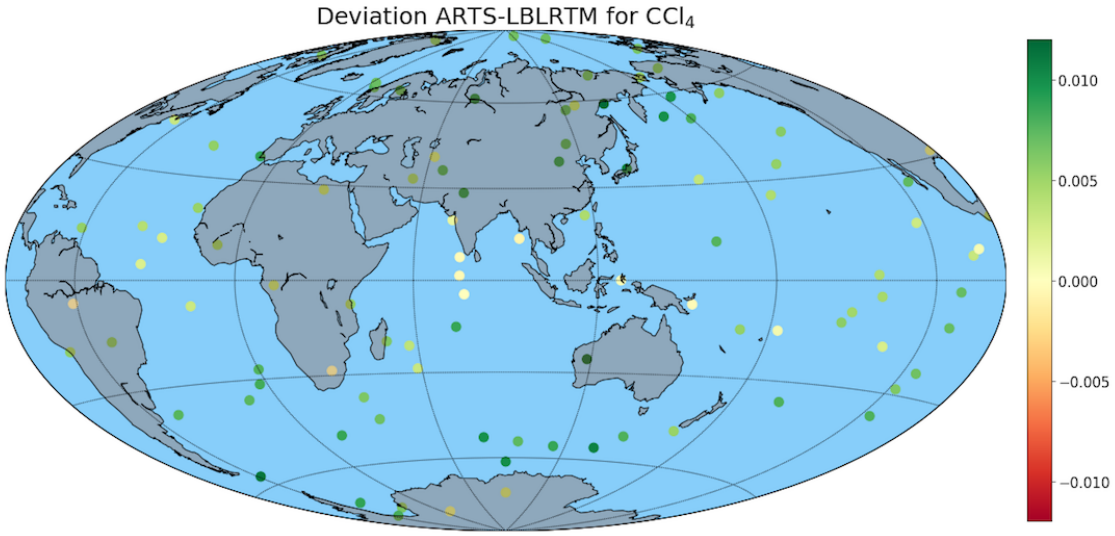

Figure 4.4: Worldmap for CCl_4.

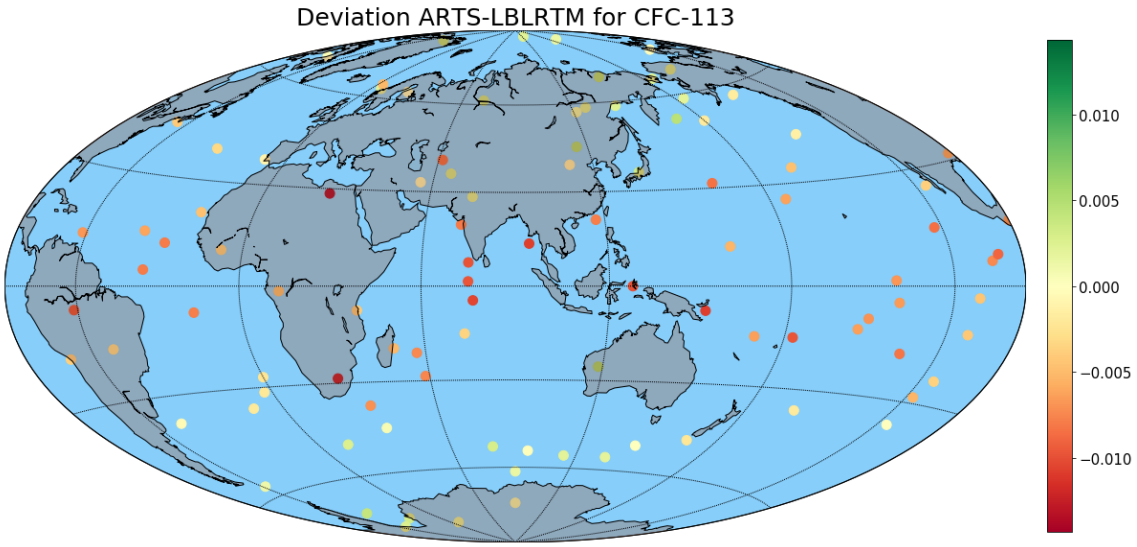

Figure 4.5: Worldmap for CFC-113.

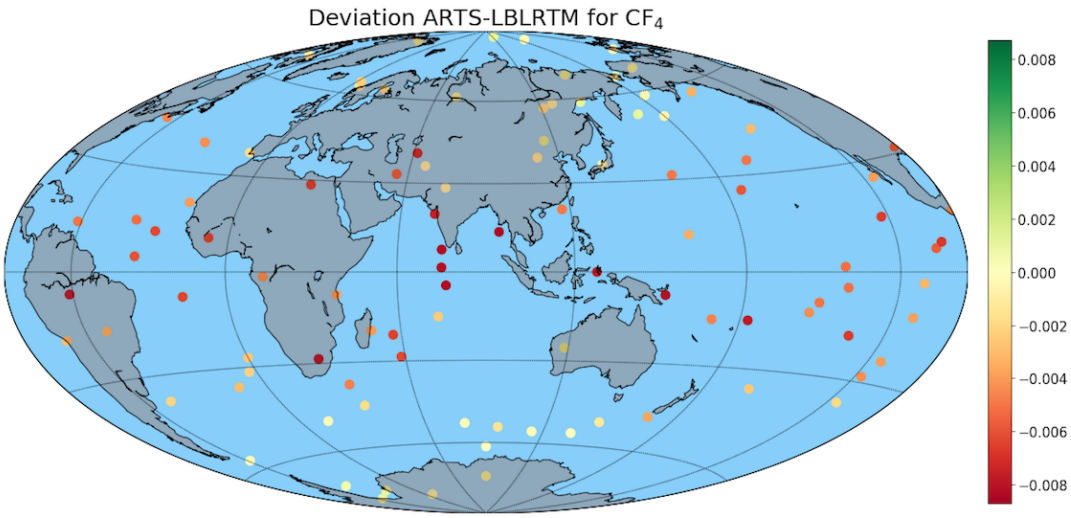

Figure 4.6: Worldmap for CF_4.

4.4.2 Spectral differences

An explanation for the discrepancy between the models and also between the atmospheres could be differences in the spectral data. In this context the spectral upwards irradiance flux at the TOA is plotted for both models and as the mean over all 100 atmospheres (see Figures 4.7 to 4.9). Shown are the spectra for every gas as calculated with both models. The bottom plots present the spectral irradiance flux in the spectral range from $500\,\mathrm{cm}^{-1}$ to $1500\,\mathrm{cm}^{-1}$. The plots for the gases CFC-12 and CFC-113 can be found in the appendix (Chapter 5). If integrated over the whole spectrum the area under the line can be interpreted as the total radiative forcing value.

The comparison for CFC-11 is shown in Figure 4.7. The radiative forcing values for CFC-11 for both models in Table 4.7 are in good agreement. The spectral features display the same good agreement although one can identify that the peaks in the LBLRTM spectra indeed have the same shape but are slightly smaller than in the ARTS spectra. The spectra for CFC-12 and CFC-113 (Figures 5.1 and 5.2) show the same good agreement which fits to the relatively small deviation in the radiative forcings. When looking at the spectra for all gases calculated with LBLRTM one notices a spike at wavenumber $2000\,\mathrm{cm}^{-1}$ which occurs in every spectrum at the same wavenumber and in a similar magnitude. This spike will be further discussed in the next paragraph. Before analysing the spike and its impact it is important to first have a look at the spectra for CCl_4 and CF_4 which had rather high deviations between the models. Figure 4.8 shows clearly that not only the spike at wavenumber $2000\,\mathrm{cm}^{-1}$ influences the forcing values for CCl_4 but

also the distinctive difference in the shape and magnitude of the spectral band located around 800 cm^{-1}. The ARTS forcing values for CCl_4 are overall higher than the LBLRTM values (see Figure 4.1) which is in line with the smaller and more narrow band shape. For CF_4 radiative forcings had the biggest differences between the models. LBLRTM forcing values were here mostly higher than the ARTS values. Figure 4.9 shows that the main band located around 1250 cm^{-1} has a similar shape in both models but the magnitude of the ARTS spectrum is – contrary to expectations – bigger than the LBLRTM spectrum even though the LBLRTM has the bigger radiative forcing value. This indicates that the abnormal spike at wavenumber 2000 cm^{-1} seems to have a big influence on the resulting radiative forcing values for CF_4.

A closer look at the conspicuous spike located at wavenumber 2000 cm^{-1} is possible in Figure 4.10. From the standard deviation one can see that the spectral irradiance and therefore the area of the spike varies between 0.02 $pW/m^2 \cdot Hz$ and 0.11 $pW/m^2 \cdot Hz$ depending on the atmosphere data. The different magnitude of the spike and therefore the different impact on the forcing values could be the reason for the difference in deviations depending on the atmosphere data as shown in Figures 4.1, 4.2, 4.3, 4.4 and 4.6. The working hypothesis is that the spike causes bigger deviations for CCl_4 and CF_4 because their radiative forcing is of a general smaller order of magnitude than the forcings of CFC-11 and CFC-12. In order to quantify the impact of the spike the radiative forcings excluding the spike were calculated by integrating over the spectrum in the range from 0 cm^{-1} to 1500 cm^{-1}. The resulting forcing values can be found in Table 4.8. The revised deviation of the forcing values for CFC-11 and CFC-12 increases slightly whereas the deviation for CFC-113 and CF_4 decreases. Especially remarkable is the fact that the ARTS forcing value for CF_4 is now, in contrast to earlier calculations, higher than the LBLRTM value. This result agrees better with the comparison of the spectra for CF_4 and underlines the impact of the spike on the resulting forcing value. Furthermore, the revised deviation for CCl_4 is striking. A percentage deviation of now -52 % matches the already mentioned differences in the spectral band around wavenumber 800 cm^{-1}. The difference between the models increases and the LBLRTM values are now even lower than the ARTS values as before.

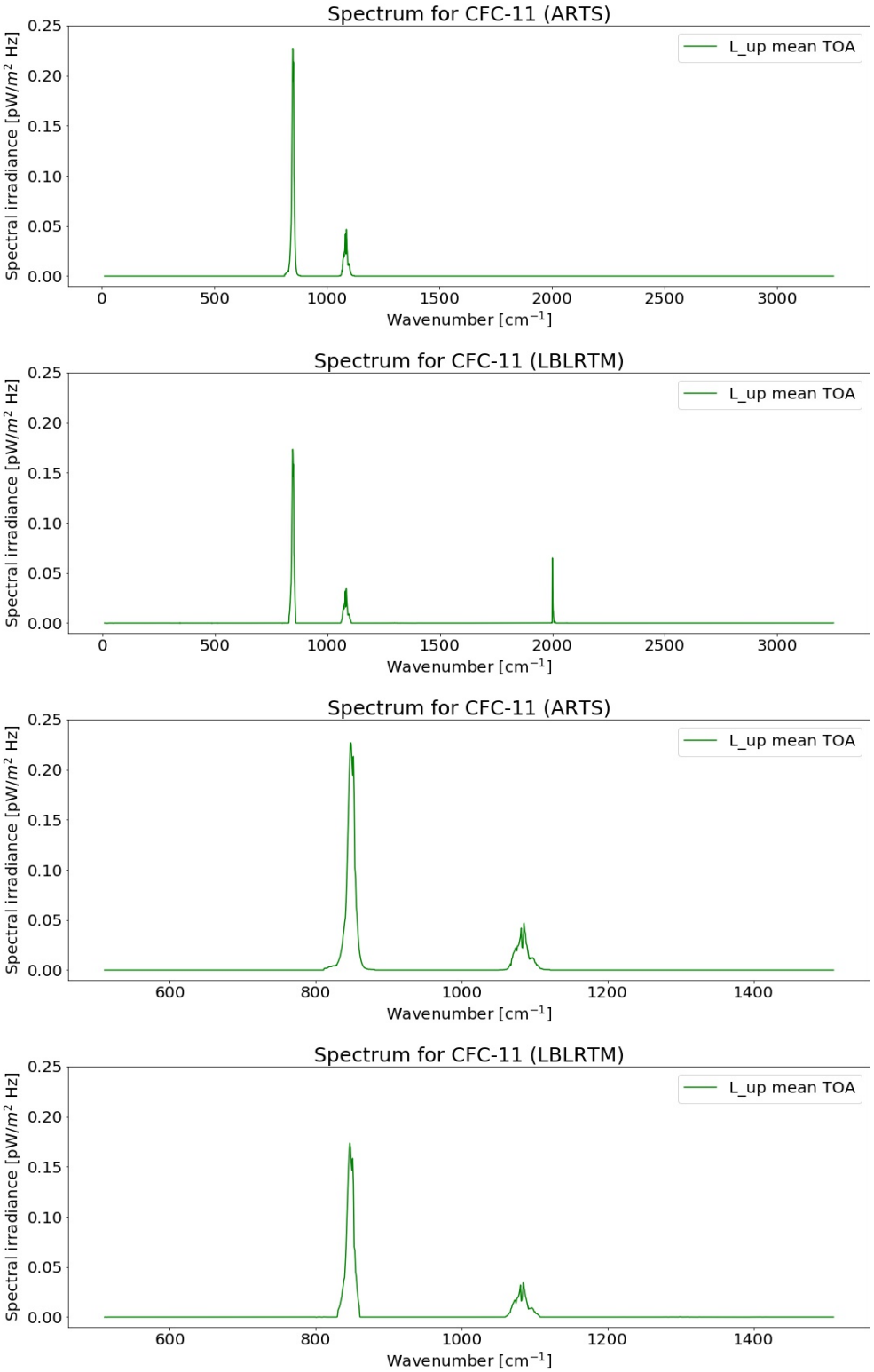

Figure 4.7: Comparison of mean spectral upwards irradiance fluxes at TOA for CFC-11 calculated by ARTS and LBLRTM. The 2 bottom plots present the spectral irradiance flux in the spectral range from 500 cm^{-1} to 1500 cm^{-1}.

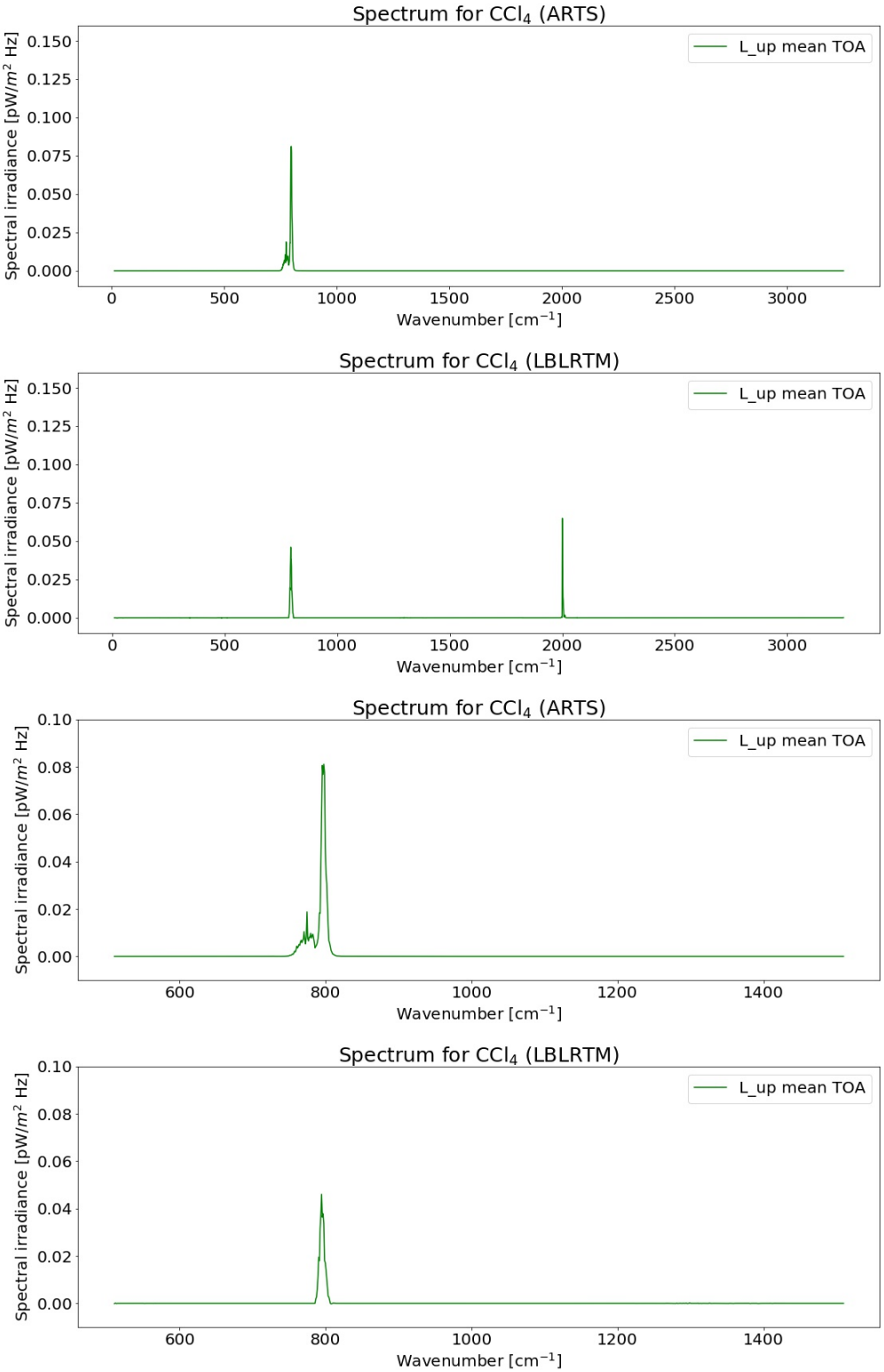

Figure 4.8: Comparison of mean spectral upwards irradiance fluxes at TOA for CCl_4 calculated by ARTS and LBLRTM. The 2 bottom plots present the spectral irradiance flux in the spectral range from 500 cm^{-1} to 1500 cm^{-1}.

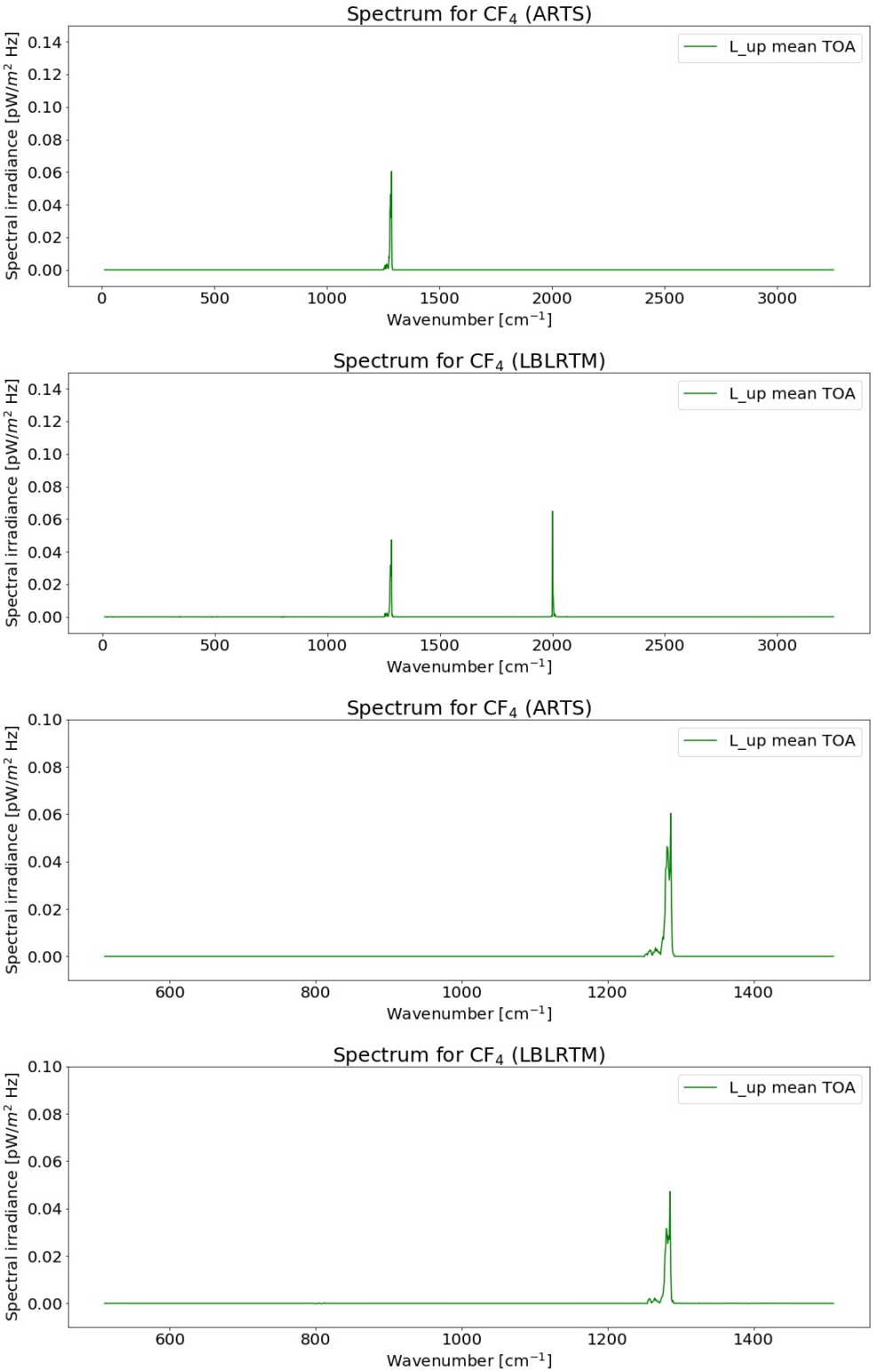

Figure 4.9: Comparison of mean spectral upwards irradiance fluxes at TOA for CF_4 calculated by ARTS and LBLRTM. The 2 bottom plots present the spectral irradiance flux in the spectral range from 500 cm^{-1} to 1500 cm^{-1}.

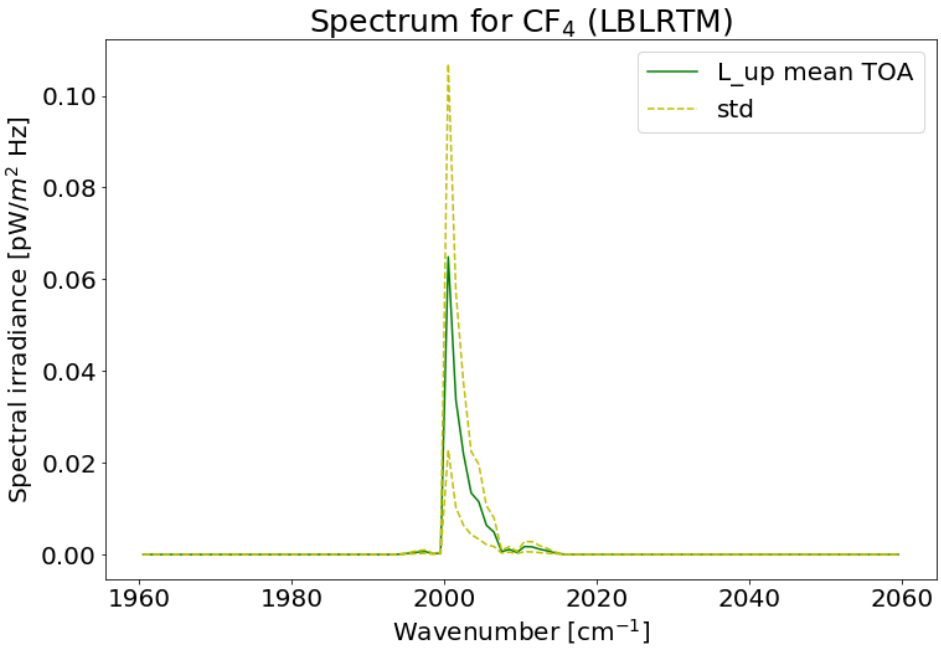

Figure 4.10: Zoom of the spike in the LBLRTM spectrum for CF_4 at 2000 cm^{-1}. The dotted green line presents the standard deviation of the spectral fluxes over the 100 atmospheres.

Table 4.8: Revised comparison of RFs calculated by ARTS and LBLRTM (instantaneous, clear-sky). The last column presents the percentage error between the 2 models for each gas.

Gas	**RF_{ARTS} [W/m^2]**	**Old RF_{LBLRTM} [W/m^2]**	**Revised RF_{LBLRTM} [W/m^2]**	**Old deviation [%]**	**Revised deviation [%]**
CFC-11	0.0941±0.0219	0.0873±0.0238	0.0795	-7.3	-15.5
CFC-12	0.2595±0.0653	0.2389±0.0668	0.2262	-7.9	-12.8
CFC-113	0.0347±0.0083	0.0381±0.0117	0.0317	9.8	-8.6
CCl_4	0.0219±0.0045	0.016±0.005	0.0105	-26.3	-52.0
CF_4	0.0107±0.0027	0.014±0.005	0.0086	32.1	-20.0

In conclusion, ARTS and LBLRTM show good consistency for the main CFCs, CFC-11, CFC-12 and CFC-113, and more striking differences for CCl_4 and CF_4. We assume that the main differences are caused by discrepancy in the spectral data and also by the spike in the spectra at wavenumber 2000 cm^{-1}. At this point, we know that the spike and the resulting error in the forcing values was caused by the use of malfunctioning line data in the LBLRTM model. But even without the impact of this spike the deviations between the 2 models remain. Nonetheless the good agreement of the 2 state-of-the-art models for the main CFCs, CFC-11 and CFC-12, indicates that the radiative forcing values for CFC-11 and CFC-12 might be higher than was assumed until now.

Chapter 5

Conclusion and Outlook

The main goal of this thesis was to validate a new gas absorption scheme which was implemented into ARTS by analysing the resulting radiative forcing values for 6 atmospheric gases. We found that the results of this validation vary a lot depending on the gas which is studied. According to the IPCC (2013) halocarbons contributed $0.337\,\mathrm{W/m^2}$ to the total adjusted radiative forcing, whereas CFC-11, CFC-12, CFC-113 and HCFC-22 account for 85 % of this forcing value. Their impact on the Earth's energy balance is therefore non-negligible and state-of-the-art calculations of their forcing contributions could be of great importance for future climate projections. Since HCFC-22 has not yet been included into ARTS, the focus of my thesis was on the chlorofluorocarbons CFC-11, CFC-12 and CFC-113. Additionally, CF_4, CCl_4 and HFC-134a were investigated but proper comparison was only possibly for the 3 CFCs, CF_4 and CCl_4.

The comparison of the radiative forcing values to IPCC and other literature values showed, that the ARTS values for CFC-11 and CFC-12 were in good agreement and deviations are assumed to be mainly caused by the use of different kinds of models and input data. The intercomparison with the RRTMG model also reflects the good conformity for CFC-11 and CFC-12. Especially the last comparison to the LBLRTM model confirms the good plausibility of the ARTS results. Deviations lie below 8 % of the ARTS value whereas ARTS estimated a higher forcing than LBLRTM. Comparisons with the other gases didn't conclude in the same conformity. The deviations for CCl_4 and CF_4 were striking, especially in the intercomparison of ARTS and LBLRTM, which were run in the same way using the same atmospheric input data. Deviations up to 32.1 % for CF_4 occurred. Further investigation into CF_4 showed, that differences in the spectral data of the 2 models most likely cause the high deviation. Additionally, we identified a strange spike around wavenumber $2000\,\mathrm{cm^{-1}}$ in the LBLRTM spectra which occurred for all gases at the same location and in similar magnitude. At this point we know that the reason for the bug in form of the spike lies in malfunctioning line data.

Revised calculations and comparisons excluding the spike result in a largely better agreement for CF_4 and slightly worse agreement for CFC-11 and CFC-12. This corroborates our hypothesis that the spike mainly influences the forcing values of gases with generally smaller forcing values.

The results of my thesis could serve as starting point for improved and more detailed comparison of the 2 models in the future. In this context, it would be helpful to in-depth examine and discuss differences in the radiative transfer calculations. Especially the application of broadening mechanisms for the different gases and the source and use of spectral information should be reviewed. Furthermore, the question of how big the influence of the temperature and pressure dependence of absorption by CF_4 is, as described in Section 4.1 could be further investigated. In this context it would be interesting to know how the temperature and pressure dependence of absorption is handled by LBLRTM and whether this might also contribute to the uncertainty in the radiative forcing values. Even though the overall influence described in Section 4.1 was fairly small for most of the gases, the temperature correction for other gases might have a non-negligible impact on the forcing values and should be further reviewed.

Concluding the intercomparison of radiative transfer models, the difference between LBLRTM and RRTMG is surprising. Both models are maintained by the Atmospheric and Environmental Research (AER) group and differ mainly in the way gas absorption is calculated. Nonetheless, one would not expect the differences in forcing values, calculated line-by-line with LBLRTM and narrowband with RRTMG, to be this big. It is further surprising that RRTMG derives the biggest forcing values for CFC-11 and CFC-12 of all 3 models. ARTS calculated the second highest values and LBLRTM the lowest for the 2 CFCs. In contrast to that the forcing values for CCl_4 calculated by RRTMG and LBLRTM are in good agreement whereas the ARTS value for CCl_4 is remarkably higher.

Regarding the main goal of my thesis I can say that in my discretion the scheme implemented into the state-of-the-arts radiative transfer model ARTS works well and produces overall reasonable results. The results of my thesis show that the impact of CFC-11 and CFC-12 in terms of radiative forcing may have been underestimated until now. Their fairly high forcing, long lifetime and ozone depleting effects underline once again the importance of the Montreal protocol in 1989. There are more halocarbons and other radiatively active atmospheric gases which have not been included into the ARTS model yet. The future goal is to further enhance and validate the scheme implemented into the ARTS radiative transfer model and to integrate more radiatively active species.

Appendix

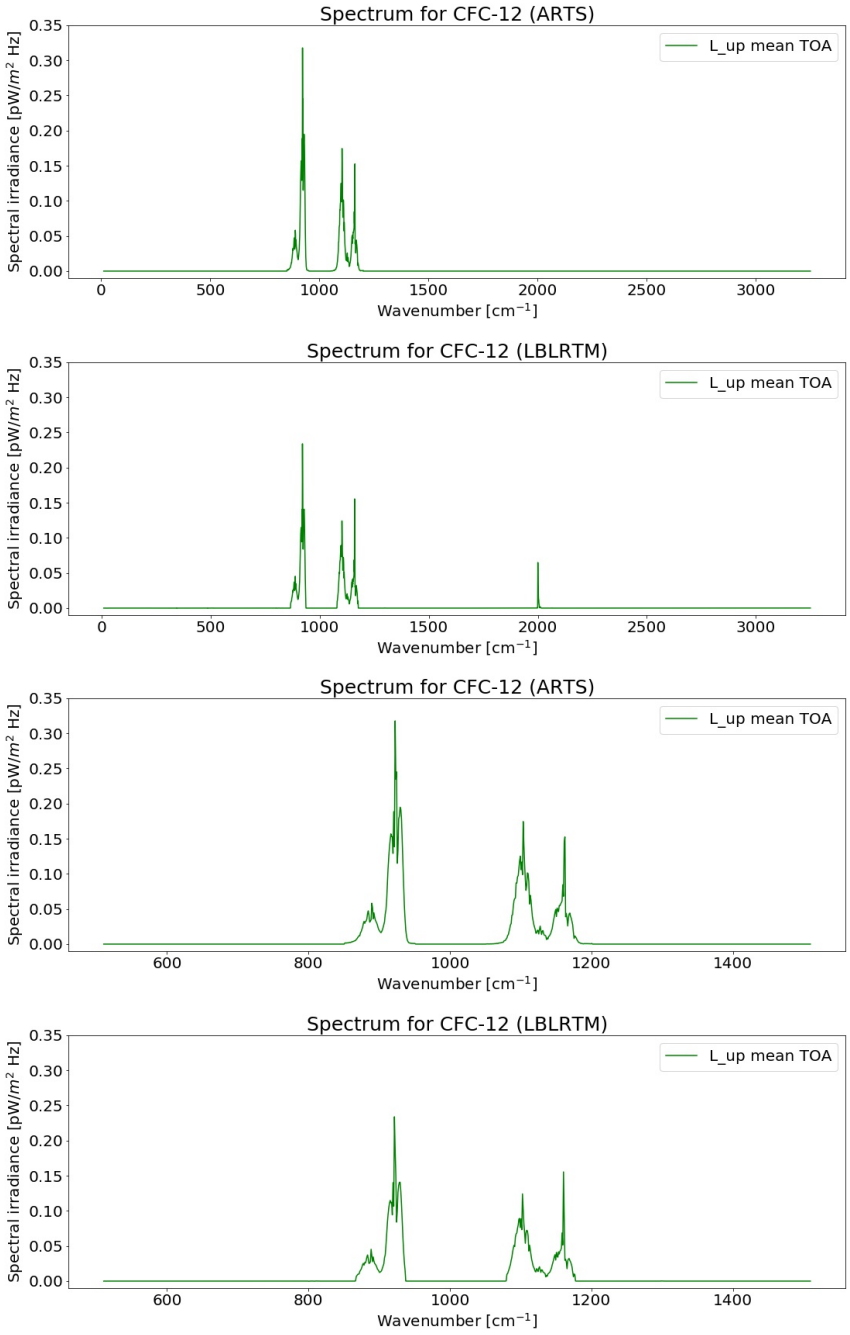

Figure 5.1: Comparison of mean spectral upwards irradiance fluxes at TOA for CFC-12 calculated by ARTS and LBLRTM.

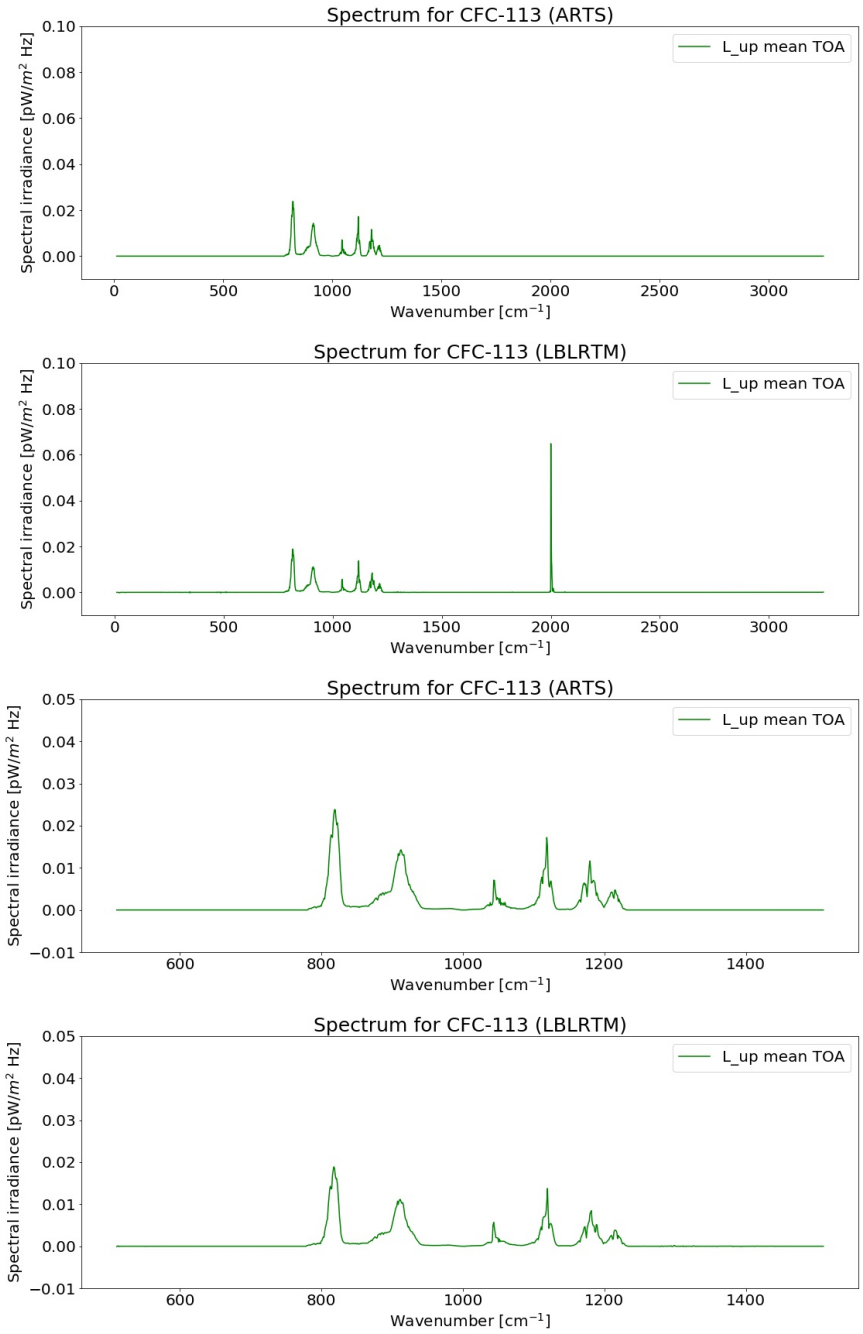

Figure 5.2: Comparison of mean spectral upwards irradiance fluxes at TOA for CFC-113 calculated by ARTS and LBLRTM.

Bibliography

Bera, P. P., Francisco, J. S., and Lee, T. J. (2009). Identifying the Molecular Origin of Global Warming. *The Journal of Physical Chemistry A*, 113(45):12694–12699. PMID: 19694447.

Buehler, S. and Eriksson, P. (2017). ARTS User Guide. `http://www.radiativetransfer.org/misc/arts-doc-stable/uguide/arts_user.pdf`. (accessed: 2018-09-17).

Buehler, S., Eriksson, P., Kuhn, T., von Engeln, A., and Verdes, C. (2005). ARTS, the atmospheric radiative transfer simulator. *Journal of Quantitative Spectroscopy and Radiative Transfer*, 91.

Calisto, M., Folini, D., Wild, M., and Bengtsson, L. (2014). Cloud radiative forcing intercomparison between fully coupled CMIP5 models and CERES satellite data. *Annales Geophysicae*, 32(7):793–807.

Christidis, N., Hurley, M., Pinnock, S., Shine, K., and Wallington, T. (1997). Radiative forcing of climate change by CFC-11 and possible CFC replacements. *Journal of Geophysical Research: Atmospheres*, 102(D16):19597–19609.

Eriksson, P., Buehler, S., Davis, C., Emde, C., and Lemke, O. (2011). ARTS, the atmospheric radiative transfer simulator, version 2. *Journal of Quantitative Spectroscopy and Radiative Transfer*, 112:1551–1558.

IPCC (1990). *Climate Change-The IPCC Scientific Assessment (1990): Report prepared for Intergovernmental Panel on Climate Change by Working Group I*. Cambridge University Press, Cambridge, United Kingdom and New York, NY, USA.

IPCC (2001). *Climate Change 2001: The Scientific Basis. Contribution of Working Group I to the Third Assessment Report of the Intergovernmental Panel on Climate Change*. Cambridge University Press, Cambridge, United Kingdom and New York, NY, USA.

IPCC (2007). *Climate Change 2007: The Physical Science Basis. Contribution of Working Group I to the Fourth Assessment Report of the Intergovernmental Panel on Climate Change*. Cambridge University Press, Cambridge, United Kingdom and New York, NY, USA.

IPCC (2013). *Climate Change 2013: The Physical Science Basis. Contribution of Working Group I to the Fifth Assessment Report of the Intergovernmental Panel on Climate Change*. Cambridge University Press, Cambridge, United Kingdom and New York, NY, USA.

Jain, A., Briegleb, B., Minschwaner, K., and Wuebbles, D. (2000). Radiative forcings and global warming potentials of 39 greenhouse gases. *Journal of Geophysical Research: Atmospheres*, 105(D16):20773–20790.

Martinerie, P., Nourtier-Mazauric, E., Barnola, J.-M., Sturges, W. T., Worton, D. R., Atlas, E., Gohar, L. K., Shine, K. P., and Brasseur, G. P. (2009). Long-lived halocarbon trends and budgets from atmospheric chemistry modelling constrained with measurements in polar firn. *Atmospheric Chemistry and Physics*, 9(12):3911–3934.

Montzka, S. and Butler, J. (2018). The NOAA Annual Greenhouse Gas Index (AGGI). `https://www.esrl.noaa.gov/gmd/aggi/aggi.html`. (accessed: 2018-08-15).

Myhre, G. and Stordal, F. (1997). Role of spatial and temporal variations in the computation of radiative forcing and gwp. *Journal of Geophysical Research: Atmospheres*, 102(D10):11181–11200.

Myhre, G., Stordal, F., Gausemel, I., Nielsen, C. J., and Mahieu, E. (2006). Line-by-line calculations of thermal infrared radiation representative for global condition: CFC-12 as an example. *Journal of Quantitative Spectroscopy and Radiative Transfer*, 97(3):317–331.

National-Research-Council (2005). *Radiative Forcing of Climate Change: Expanding the Concept and Adressing Uncertainties*. The National Academies Press, Washington, D.C.

Petty, G. W. (2006). *A First Course In Atmospheric Radiation*. Sundog Publishing, second edition.

Pincus, R., Forster, P. M., and Stevens, B. (2016). The Radiative Forcing Model Intercomparison Project (RFMIP): experimental protocol for CMIP6. *Geoscientific Model Development*, 9(9):3447–3460.

Pinnock, S., Hurley, M., Shine, K., Wallington, T., and Smyth, T. (1995). Radiative forcing of climate by hydrochlorofluorocarbons and hydrofluorocarbons. *Journal of Geophysical Research: Atmospheres*, 100(D11):23227–23238.

Sihra, K., D. Hurley, M., P. Shine, K., and J. Wallington, T. (2001). Updated radiative forcing estimates of 65 halocarbons and nonmethane hydrocarbons. 106:20493–20505.

Singh, H., Tiwari, L., and Rao, D. P. (2014). Computational study on OH and Cl initiated oxidation of 2,2,2-trifluoroethyl trifluoroacetate (CF3C(O)OCH2CF 3). *Bulletin of the Korean Chemical Society*, 35:1385–1390.

Acknowledgements

I wish to express my sincere thanks to everyone who was involved in the development of this bachelor thesis. First and foremost, I would like to especially thank my supervisors Prof. Stefan Bühler and Manfred Brath, who supported and guided me throughout my thesis and constantly provided their expertise on the topic. Their reachability and open door policy was very appreciated.
Furthermore, I would like to thank Manfred Brath, Lukas Kluft and Oliver Lemke for their assistance with ARTS and Python and their patience while doing so.
I would also like to express my gratitude to Eli Mlawer and his team for providing me with data from the LBLRTM which I used in the intercomparison and improved the validity of my thesis.
A special thank is dedicated to my mother and my fellow students Lukas, Philine and Theresa for proofreading my thesis and giving valuable feedback.
Last but not least I would like to thank my parents and my friends for their support and encouragement through this challenging phase of life.

Eidesstattliche Versicherung

Hiermit versichere ich an Eides statt, dass ich die vorliegende Arbeit im Studiengang BSc. Meteorologie selbstständig verfasst und keine anderen als die angegebenen Hilfsmittel – insbesondere keine im Quellenverzeichnis nicht benannten Internet–Quellen – benutzt habe. Alle Stellen, die wörtlich oder sinngemäß aus Veröffentlichungen entnommen wurden, sind als solche kenntlich gemacht. Ich versichere weiterhin, dass ich die Arbeit vorher nicht in einem anderen Prüfungsverfahren eingereicht habe und die eingereichte schriftliche Fassung der auf dem elektronischen Speichermedium entspricht. Ich bin zudem damit einverstanden, dass die Bachelorarbeit veröffentlicht wird.

Hamburg, den 11. November 2018 _____